RELATIVE PERFORMANCE OF CC6 CONCRETE PAVEMENT TEST ITEMS AT THE FAA NATIONAL AIRPORT PAVEMENT TEST FACILITY

By:
David R. Brill
FAA Airport Technology R&D Branch, ANG-E262
William J. Hughes Technical Center
Atlantic City International Airport, NJ 08405
USA
Phone: (609) 485-5198; Fax: (609) 485-4845
David.Brill@faa.gov

And
Izydor Kawa
SRA International, Inc.
Linwood, New Jersey
USA

PRESENTED FOR THE
2014 FAA WORLDWIDE AIRPORT TECHNOLOGY TRANSFER CONFERENCE
Galloway, New Jersey, USA

August 2014

ABSTRACT

Between August 2011 and April 2012, six rigid pavement test items, designated CC6, were trafficked to full structural failure at the Federal Aviation Administration (FAA) National Airport Pavement Test Facility (NAPTF). The primary objective of these full-scale tests was to investigate the effect on pavement life of concrete flexural strengths higher than recommended by current FAA standards in Advisory Circular (AC) 150/5320-6E. The six test items were constructed using three different concrete mixes with different flexural strengths. All test items were subjected to traffic from 4-wheel landing gears in a 2D configuration. Pavement condition was continuously monitored, and traffic was continued until the structural condition index (SCI) of all test items was under 30, which is well below the design failure condition of SCI 80. Due to the significantly different flexural strengths, it was necessary to vary the gear loads to achieve failure of all test items in a reasonable number of traffic passes. Moreover, all test items (except one) received traffic at a mixture of different load levels. Therefore, in order to compare test item performance, it was necessary to introduce mixed aircraft traffic concepts to the analysis. A rational method of compensating for various load levels, making use of the cumulative damage factor (CDF), results in equivalent traffic passes to failure at a reference wheel load, so that the effect of concrete strength can be clearly observed. Using this method, it was demonstrated that CC6 pavement life was strongly correlated to 28-day flexural strength, and was not strongly affected by the base type.

INTRODUCTION

The sixth construction cycle at the FAA NAPTF (designated CC6) was designed and executed to address several questions related to the performance of rigid airport pavements. The key question for this construction cycle concerned the relative effect of concrete flexural strength on pavement life. Specifically, will concrete that is "too strong" perform poorly due to a tendency to fracture at low energy (brittleness)? In the technical literature on concrete fracture, high-strength concrete is associated with increased brittleness relative to normal concrete. As stated by Bažant and Planas [1], "High strength concrete (HSC) is known to be more brittle than normal strength concrete (NC). This is so because c_f is smaller for HSC, and then, for a given geometry $D_0^{HSC} < D_0^{NC}$." In the preceding, c_f is defined as the effective length of the fracture process zone (a concrete material property measuring deviation from linear elastic fracture mechanics), and D_0 refers to a size effect parameter. In 2007, an FAA-sponsored report of the Innovative Pavement Research Foundation (IPRF) noted that "very high strength concrete can be brittle and result in lower fatigue life," and therefore recommended that the FAA's P-501 concrete specification be modified to require FAA approval of design concrete strengths above 650 psi [2]. While this IPRF recommendation was not fully adopted by the FAA, the current Advisory Circular (AC) on pavement design, AC 150-5320-6E, nevertheless recommends that design strength should be kept between 600 and 700 psi "for most airport applications" [3]. In practice, concrete in this strength range is not always locally available, which can lead to considerable overdesign of rigid slabs. Furthermore, there is little hard evidence that any specific concrete strength value (such as 700 psi) is associated with reduced fatigue life in the field. The apparent embrittlement of particular pavements containing relatively high-strength concrete may be related to other factors, such as excessively high cement content, too low water/cement (w/c) ratio, or improper construction procedures, that can be controlled outside of the structural design

procedure. In view of the above, the main purpose of CC6 was to compare the performance of full-scale rigid pavements constructed with high-strength concrete mixes to pavements similar in all respects, except with concrete in the FAA recommended strength range.

A second main test objective was to investigate the effect of the stabilized subbase material on pavement performance. Specifically, would rigid pavements constructed on stiffer platforms (e.g., econocrete, or "lean" concrete) prove more susceptible to top-down cracks than similar pavements on less stiff (asphalt stabilized) bases? For this purpose, three of the six test items were constructed on econocrete (FAA Item P-306) bases, and the other three test items were on hot-mix asphalt (HMA) bases.

In addition to the two main test objectives, there was a subsidiary experiment conducted under CC6 comparing two different types of rigid pavement isolation joints (thickened-edge and reinforced) that both conform to current FAA design standards [3]. The results of the joint comparison test are outside the scope of this paper, but they are discussed in another paper by Brill and Wang [4].

NATIONAL AIRPORT PAVEMENT TEST FACILITY (NAPTF)

Testing was conducted at the NAPTF, located at the FAA William J. Hughes Technical Center in New Jersey, USA. The NAPTF, opened in 1999, is a unique facility for full-scale testing of airport pavements. Simulated aircraft gear loads are applied to the pavement via a rail-based test vehicle propelled by sixteen variable-frequency electric drive motors. As shown in Figure 1, the vehicle has two carriages, a north carriage and a south carriage, each of which can be separately configured to simulate a full-scale aircraft landing gear of up to ten wheels. Each carriage can be wandered independently. Vertical loads are produced by ten hydraulic-actuated load modules, five modules on each carriage. Depending on the number of modules in operation at any time, the vehicle may impart loads of up to 75,000 lbs. per wheel, up to a total load of approximately 1.1 million pounds (i.e., the weight of the vehicle frame plus ballast). At the time of CC6 testing, the servo-hydraulic controls were able to maintain the wheel loads within approximately 2 percent of the set value.

CC6 EXPERIMENTAL DESIGN

CC6 consisted of six rigid pavement test items, as shown in plan in Figure 2. The cross-sectional properties the test items are given in Table 1. North and south test items were of identical cross section except for the stabilized base material. The specification items in Table 1 (e.g., P-501) refer to corresponding items as given in FAA AC 150/5370-10F [5]. Generally, the material provisions of reference [5] were adhered to, except where specific deviations (e.g., exceeding the allowable w/c ratio) were allowed for experimental reasons. All test items were constructed on a Dupont clay subgrade, placed wet of optimum to produce a mean CBR at the top of the subgrade of 6.9. Plate load tests conducted at the top of the subgrade, using the test vehicle frame as a reaction force, yielded average *k*-values of 136 pci and 150 pci for the north side and south side, respectively.

Figure 1. The NAPTF Test Vehicle.

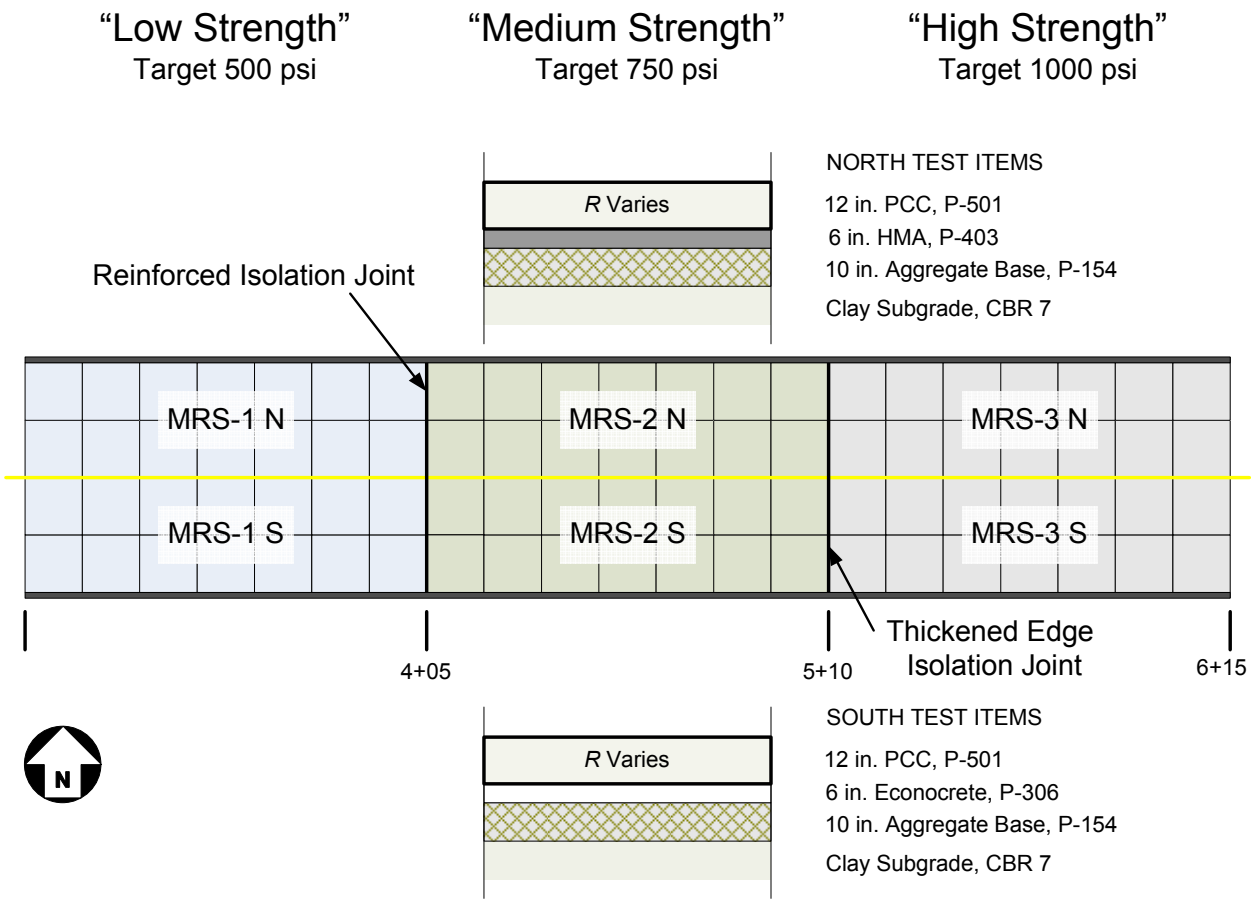

Figure 2. CC6 test Item Layout.

In Figure 2, the six test items are identified by a code starting with "MRS." This code identifies the test item as being on medium-strength subgrade ("M"), of rigid construction ("R") and with a stabilized base material ("S"). The numbers 1, 2 and 3 correspond to low-, medium- and high-strength concrete respectively, while suffixes "N" and "S" refer to north and south test items.

Table 1.
Cross-Sectional Properties of CC6 Test Items.

Layer Type	North Test Items	South Test Items
Surface	12 in. (305 mm) PCC, P-501	12 in. (305 mm) PCC, P-501
Base	6 in. (152 mm) HMA, P-403	6 in. (152 mm) Econocrete, P-306
Subbase	10 in. (254 mm) Aggregate, P-154	10 in. (254 mm) Aggregate, P-154
Subgrade	Clay Subgrade, CH, CBR 7	Clay Subgrade, CH, CBR 7

Each test item consisted of a 2 × 7 array of 15 × 15 ft. slabs. All slabs were constructed using fixed forms and were doweled both longitudinally and transversely, except at the isolation joints. Although 15-ft slabs are atypical in new construction, these dimensions were used to maintain the maximum joint spacing recommended in AC 150/5320-6E [3], and thereby minimize the risk of significant slab curling. The last row of slabs adjacent to either the test pavement end, or an isolation joint, was considered part of a transition area and was discounted for the purpose of evaluating performance. Therefore, only the interior group of 10 slabs for each test item was used to compute pavement condition index (PCI) and structural condition index (SCI).

As stated above, the concrete strength was the key experimental variable. The FAA team devoted considerable effort to designing concrete mixes giving significantly different levels of flexural strength when tested in the laboratory by ASTM Test Method C78 (standard four-point beam flexural strength test) [6]. Table 2 compares the target and as-placed flexural strength values for the three concrete mixes designated as low-strength, medium-strength and high-strength. As indicated in Table 2, the final as-placed 28-day strength for the low-strength mixture (662 psi) was higher than the original target strength of 500 psi. Nevertheless, the higher value was deemed experimentally acceptable as it was still low enough to produce a statistically significant separation from the medium-strength concrete. The medium- and high-strength mean 28-day flexural strength values were close to the target values of 750 and 1000 psi, respectively. Different materials and proportions were used to obtain the various concrete strengths. The different placement concrete mixes are listed in Table 3. Note that the coarse and fine aggregates and other material sources for the medium- and high-strength mixes are the same; the difference between the two stronger mixes is the proportioning, in particular the cement content and w/c ratio. The coarse aggregate in the stronger mixes (a blend of Penn Jersey No. 57 and No. 8 stones) was primarily limestone with some quartzite and chert. By contrast, the coarse aggregate used in the low-strength mix (Harmony No. 57) was a rounded river rock, primarily quartzite and sandstone, obtained from the Berks quarry in northwestern New Jersey. From Table 3 it can be seen that the lower strength of the 500 psi target strength mix relative to the 750 psi mix resulted from a combination of factors: lower quality aggregates, less cement and higher w/c ratio. All three mixes used all Portland cement as binder; fly ash was not used.

Table 2.
Concrete Flexural Strength for CC6 Test Items.

Test Items	Target Flexural Strength, psi	Mean 28-day Flexural Strength, psi	Standard Deviation of 28-day strength, psi
MRS-1	500	662	48
MRS-2	750	763	113
MRS-3	1000	1007	150

Table 3.
Concrete Placement Mix Designs for CC6 Test Items[a].

Material	Low-Strength (Target 500 psi)	Medium-Strength (Target 750 psi)	High-Strength (Target 1000 psi)
Harmony No. 57 Stone, round, lbs.	1550	N/A	N/A
Penn-Jersey No. 57 Coarse Aggregate, lbs.	N/A	1475	1535
Penn-Jersey No. 9 Intermediate Coarse Aggregate, lbs.	N/A	490	535
Harmony Concrete Sand, lbs.	1414	N/A	N/A
Penn-Jersey Concrete Sand, lbs.	N/A	1225	1070
Water, lbs.	325	230	236
Portland Cement, Type I, lbs.	460	500	680
Air, percent	6.5	7.0	4.5
Air Entraining Admixture, oz.	4.5	5.0	4.5
Target Slump, in.	6.0	5.5	3.5
w/c ratio	0.71	0.46	0.35

[a]All quantities are per cubic yard of concrete

The as-placed concrete strengths reported in Table 2 were based on beam samples taken at the time of construction and tested in the laboratory using ASTM C78. In addition to the samples taken for construction acceptance, a large number of beams and cylinders from each test item was collected and stored for a parallel program of strength and beam fatigue testing. The total number of cast concrete beams set aside at placement for subsequent strength and fatigue testing using the C78 apparatus was 240 (80 for each mix).

CC6 TRAFFIC HISTORY

After construction of the CC6 test items was completed in June 2011, a series of preliminary tests was conducted on test item MRS-1 North. Only 6 out of the 10 MRS-1 North slabs were loaded in this preliminary phase, which included limited traffic testing at zero wander. These tests are separately discussed in Guo *et al*. [7], and are relevant to this paper insofar as the traffic analysis had to be adjusted to account for damage to the slabs resulting from the preliminary tests. The total traffic applied to the CC6 test items from July 2011 through April 2012, including the preliminary traffic, is summarized in Table 4. All passes were made using a 4-wheel (2D) gear load configured as shown in Figure 3, so the wheel loads in Table 4 should be multiplied by four to obtain the total gear load. Note that Table 4 refers to the number of wander patterns for each phase of loading. Except for the preliminary (zero wander) phase, traffic was applied using a repeated vehicle wander pattern consisting of 66 lateral positions on 9 discrete tracks, resulting in a lateral distribution of traffic approximating normal wander, with a wander width of 70 inches (i.e., the lateral width statistically encompassing 75 percent of traffic passes in a true normal distribution). For example, wander pattern no. 1 included passes 1 through 66; wander pattern no. 2, passes 67 through 132, and so forth. Equal passes were applied to the North and South test items (again, with the exception of the preliminary traffic applied to MRS-1 North, but not MRS-1 South).

Throughout the traffic phase, the structural performance of test items was monitored and quantified by means of the Structural Condition Index (SCI). SCI is a modification of the Pavement Condition Index (PCI) for Airports (rigid) method following ASTM D 5340 [8]. Like PCI, SCI is based on visual inspection of the pavement surface and identification of standard distresses. The difference is that in the SCI only distresses related to structural loading are counted, while environmental and construction/material-related distresses are disregarded. The specific distresses counted in the SCI are: corner breaks, longitudinal/transverse/diagonal cracks, shattered slabs, joint spalls and corner spalls. “Shrinkage cracks” are also enumerated in the SCI, but only to the extent that they represent evolving structural cracks that have not yet progressed to completion. Otherwise, distress densities, severities and methods of counting are all as described in reference [7]. In the field, pavements are divided into “sample units,” and a subset of sample units is then randomly selected for inspection. Due to the small size of CC6, each test item was considered to constitute one sample unit, and 100% inspection (i.e., of 10 slabs) was performed.

Including the preliminary loads, all test items except MRS-1 South experienced traffic at a mixture of different load levels. As shown in Table 4, the total number of passes applied to MRS-2 and MRS-3 for the duration of the experiment was 39,270. However, these passes were applied at three distinct load levels, so these test items effectively were subject to mixed traffic. The reason for using different load levels was the necessity of failing both low-strength and high-strength test items within a reasonable period of time. This is generally not possible using a unique load, because a wheel load sufficiently large to produce gradual fatigue failure in high-strength concrete may well cause low-strength concrete slabs to break immediately. Thus, to compare performance of the different test items in a meaningful way, it was necessary to compensate for the different load levels through an analytical procedure. The development of this compensation procedure is discussed in the following section.

Table 4.
CC6 Traffic History.

Dates	Wander Patterns	Wheel Load, lbs.	Passes MRS-1 N	MRS-1 S	MRS-2	MRS-3
8 July 2011 – 15 Aug 2011	N/A	44,000	6,970	0	0	0
30 Aug 2011 – 20 Dec 2011	1 – 238	45,000	15,708	15,708	15,708	15,708
27 Dec 2011 – 29 Feb 2012	239 – 405	52,000	0	0	11,022	11,022
29 Feb 2012 – 30 Mar 2012	406 – 508	52,000 70,000	0 0	0 0	6,978 0	0 6,798
30 Mar 2012 – 25 Apr 2012	509 – 595	70,000	0	0	5,742	5,742
Total Passes:			22,498	15,708	39,270	39,270

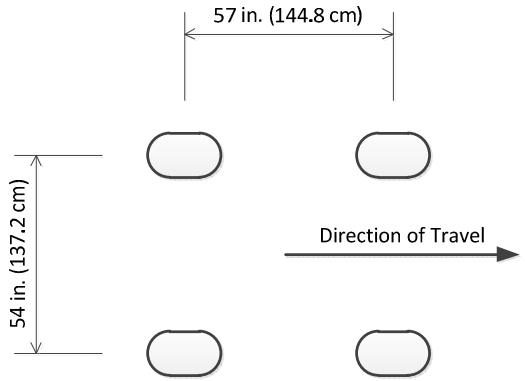

Figure 3. 2D Gear Footprint for CC6 Traffic.

The initial traffic wheel load for CC6 was based on a preliminary analysis of beam fatigue tests for the low-strength mix, performed as part of the preliminary test phase. A subgroup of the retained beams (12 beams) from the low-strength mix were tested in both strength and fatigue, from which it was determined that a load ratio (ratio of testing load to cracking load) of 80% for MRS-1 test items would give a reasonable fatigue life. After determination of the cracking load experimentally during the preliminary test phase, the initial traffic wheel load was set at 45,000 lbs. as indicated in Table 1. Details are given in reference [7].

At the beginning of the traffic test, all six test items were trafficked at the 45,000-lb. wheel load level. After 15,708 passes, the two low-strength test items had both failed, but the medium- and high-strength test items were essentially undamaged (as measured by SCI). Therefore, traffic was stopped on MRS-1, but continued on MRS-2 and MRS-3 at an increased load level of 52,000 lbs. per wheel. After an additional 11,022 passes (167 wander patterns) at the increased level, it was clear that while both sides of MRS-2 were deteriorating under traffic, the high-strength MRS-3 test items were not. Therefore, the wheel load on MRS-3 only was increased to

70,000 lbs. After an additional 6,798 passes (103 wander patterns) at the split load level, the load on MRS-2 was also increased to 70,000 lbs. Finally, after 5,742 more passes (87 wander patterns) in which both MRS-2 and MRS-3 test items received the maximum wheel load, all test items were determined to have SCI less than 40 (i.e., complete structural failure characterized by shattered slabs). At this, point, traffic was stopped. Figure 4 shows the raw data of SCI versus number of passes for all test items, uncorrected for load.

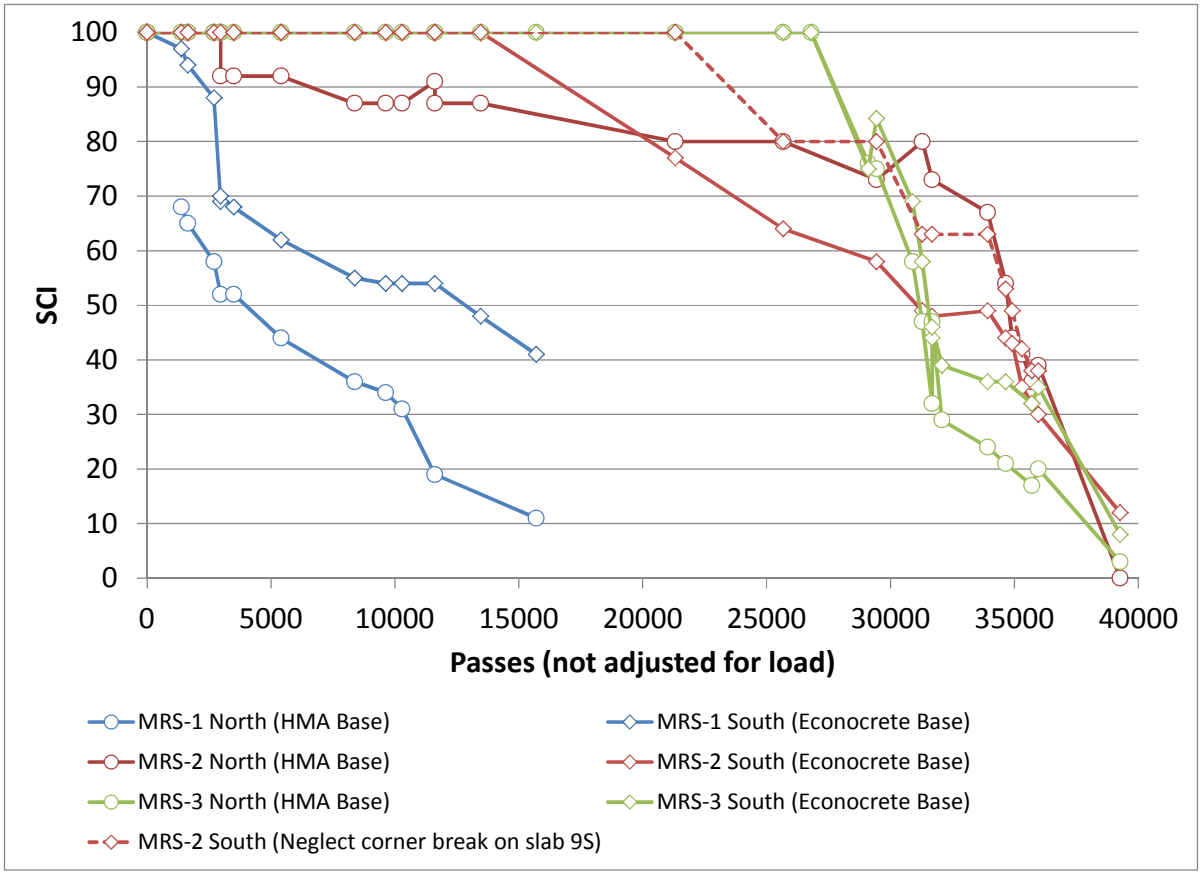

Figure 4. SCI as a function of traffic passes (all test items).

LOAD COMPENSATION PROCEDURE

Because passes have not been adjusted for load, the plot in Figure 4 does not give a clear picture of the relative performance of the test items. The procedure used here to compensate for the varying load is based on a similar procedure for flexible pavements by Hayhoe and Kawa [9]. In the flexible procedure, compensation was also needed for temperature effects, which are not relevant in the present case.

The basis of the compensation procedure is to assume the rigid failure model takes the form:

$$C_F = A \times 10^{B\left(\frac{R}{\sigma}\right)} \quad (1)$$

where: C_F = coverages to failure (where failure is defined as some value of SCI); R = concrete flexural strength; σ = computed slab stress; and A and B are fitting constants (parameters). The rigid failure model in the FAA pavement thickness design program FAARFIELD [10] can be reduced to this basic form. For mixed aircraft traffic, the cumulative damage factor (CDF) is expressed as:

$$CDF = \sum_{i=1}^{N} \frac{C_i}{C_{Fi}} \tag{2}$$

where: C_i is the actual number of coverages for aircraft i, C_{Fi} is the number of coverages to failure for aircraft i as computed from Eq. (1), and N is the number of aircraft considered. By definition, failure of the pavement occurs when CDF = 1. Therefore, for a given traffic mix known to cause failure, the problem is to find values of parameters A and B that satisfy the condition CDF = 1. This can be done in various ways, but the simplest approach is to hold B constant and find A that satisfies the failure condition.

For the CC6 traffic test, the number of "aircraft," i.e., distinct combinations of gear geometry and load, is N= 3. Each load level is treated in the model as a separate aircraft, and the number of coverages to failure for that load level calculated by means of Eq. (1). Then the model parameters are determined using Eq. (2). Once the failure model parameters are determined, the next step is to select an appropriate reference wheel load and determine the equivalent number of coverages of the trafficking gear at that wheel load that would cause failure. This step must be done by trial and error as illustrated in the following example.

Consider the example of test item MRS-3 North, whose regressed performance curve is shown in Figure 5. Also, assume that, for purposes of comparison between test items, the failure condition is SCI 50. As shown in Fig. 5, the total number of passes to the SCI 50 condition is 31,421, which includes traffic at the 45,000, 52,000 and 70,000 lb. load levels. Table 5 lists the number of unadjusted passes at each load level, and the computed stress associated with those load levels, that contributed to the failure. Stresses in Table 5 are the maximum concrete bending stresses computed by FAARFIELD, version 1.4, for the "North Test Item" structure in table 1.

Table 5.
Calculation of Coverages to Failure (SCI 50) Condition for Test Item MRS-3 North.

Wheel load, lbs.	Passes	Stress, psi[a]	Pass/Coverage[a]	Coverages
45,000	15,708	σ_1 = 506.3	4.44	C_1 = 3538
52,000	11,022	σ_2 = 572.6	4.13	C_2 = 2669
70,000	4,691	σ_3 = 734.2	3.57	C_3 = 1314

[a] computed using FAARFIELD 1.4

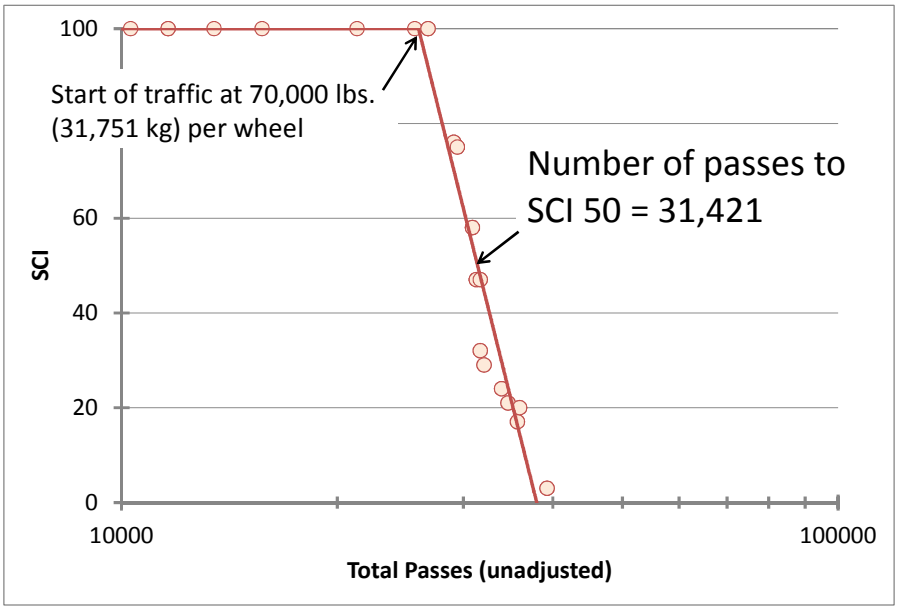

Figure 5. SCI as a function of total passes for test item MRS-3 North.

Using Eq. (2), the data in Table 5 may be fitted to the assumed failure model. At failure:

$$CDF = 1.0 = \frac{C_1}{C_{1F}} + \frac{C_2}{C_{2F}} + \frac{C_3}{C_{3F}} = \frac{1}{A} \times \left[\frac{C_1}{10^{\left(\frac{B \times R}{\sigma_1}\right)}} + \frac{C_2}{10^{\left(\frac{B \times R}{\sigma_2}\right)}} + \frac{C_3}{10^{\left(\frac{B \times R}{\sigma_3}\right)}} \right] \quad (3)$$

Substituting R = 1000 psi (the nominal concrete strength for Test Item MRS-3 North), B = 6.25 (from the FAARFIELD 1.4 model with SCI = 50 at failure), and the other variables from Table 5, Eq. (3) is solved to obtain $A = 4.07 \cdot 10^{-6}$. Note that A and B are dimensionless parameters, and do not depend on the system of units (since the units of R and σ cancel out in Eq. (3)).

Once the failure model has been completely defined, the next step is to calculate the equivalent number of passes adjusted to the 70,000-lb. reference wheel load. This is done by holding A and B constant, substituting σ_3 = 734.2 psi for the stress value in each term of Eq. (3), and adjusting the number of coverages until the value of each term of Eq. (3) matches the previous step (and CDF = 1.0). The result of the procedure for Test Item MRS-3 North is shown in Table 6. The equivalent number of passes at 70,000 lbs. per wheel, which accounts for the cumulative damage due to traffic applied at lower loads, is 1325 coverages × 3.57 = 4,731 passes, which is only slightly more than the actual passes at that load level. The equivalent passes to failure for all six test items, calculated using the above procedure for two reference load levels (45,000 lbs. and 70,000 lbs.), are listed in Table 7. The following items apply to the equivalent passes calculated in Table 7:

1. The number of total passes to the SCI = 50 condition was estimated based on linear regression of the falling portion of the SCI-versus-passes curve, where passes are plotted on a log scale, as shown in Figure 5. The regression lines are for all six test items are shown in Figure 6. A certain amount of judgment was needed in analyzing these curves,

especially where, as in MRS-2 North (Figure 6c), there was not a sharp transition from the flat to the falling portion of the curve.

2. In the case of MRS-2 South, an early corner break appeared on one slab (9S) at about 21,000 passes (see Figure 4). Because this corner break was judged to be related to construction defects rather than to applied traffic, it was disregarded for the purpose of computing equivalent passes. This resulted in a higher SCI for that test item, and more passes to failure, than would have been calculated if all distresses had been counted.

3. The preliminary traffic on Test Item MRS-1 North was accounted for in a way similar to the other cases of mixed traffic, by converting the 6,790 passes at 44,000 lbs. per wheel to equivalent passes at the reference wheel load. For the preliminary traffic, one pass was considered equivalent to one coverage (because no wander was used). It is recognized that this is an imperfect solution because: (a) all ten slabs were not trafficked under the zero-wander traffic, and (b) it ignores the static loads that were also applied to particular slabs (in some cases up to the cracking load). However, given the large uncertainties in all the variables involved, it seems to be a reasonable approach to analyzing the failure of a prematurely damaged test item.

4. The information shown in Table 7 is slightly different from unpublished preliminary data presented by Brill in 2012 [11]. The new data in this paper reflect final SCI values and a reanalysis based on the FAARFIELD 1.4 model.

Table 6.
Calculation of Equivalent Coverages at 70,000 lbs. per Wheel for MRS-3 North.

Wheel Load, lbs.	Actual Coverages	Equivalent Coverages (at 70,000 lbs. per Wheel)
45,000	3538	0.5
52,000	2669	10.5
70,000	1314	1314
Total	7521	1325

Table 7.
Equivalent Passes to Failure (SCI 50).

Test Item	Failure Model Parameters A, B	Equivalent Passes at 45,000 lbs. per wheel	Equivalent Passes at 70,000 lbs. per wheel
MRS-1 North	$5.73 \cdot 10^{-5}$, 6.25	35,653	85
MRS-1 South	$1.53 \cdot 10^{-5}$, 6.25	11,136	25
MRS-2 North	$1.14 \cdot 10^{-4}$, 6.25	915,500	985
MRS-2 South	$1.27 \cdot 10^{-4}$, 6.25	1,215,000	1,224
MRS-3 North	$4.07 \cdot 10^{-6}$, 6.25	39,903,000	4,731
MRS-3 South	$4.33 \cdot 10^{-6}$, 6.25	53,732,000	5,832

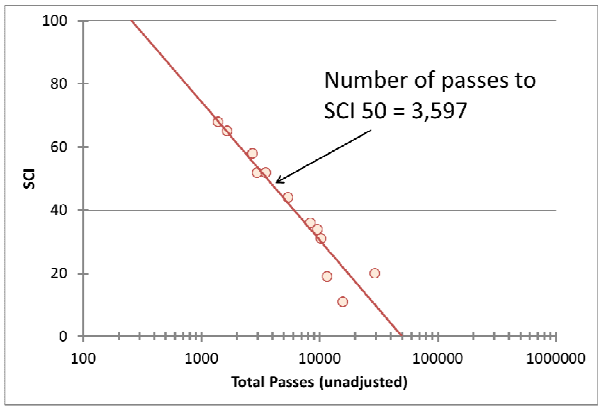

(a) MRS-1 North

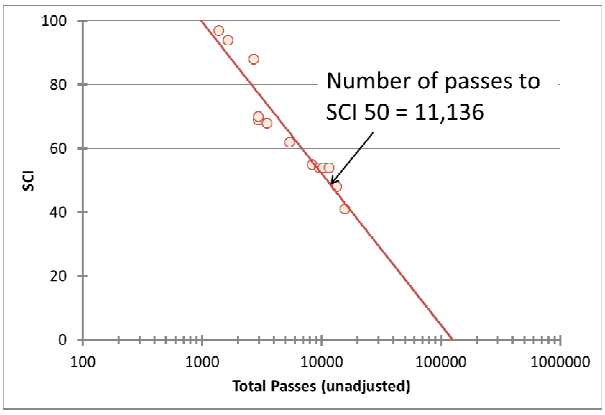

(b) MRS-1 South

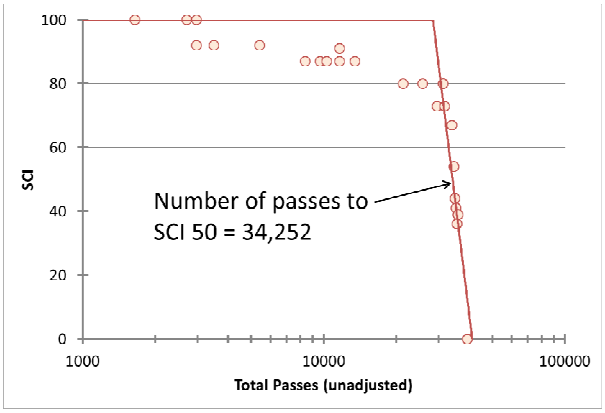

(c) MRS-2 North

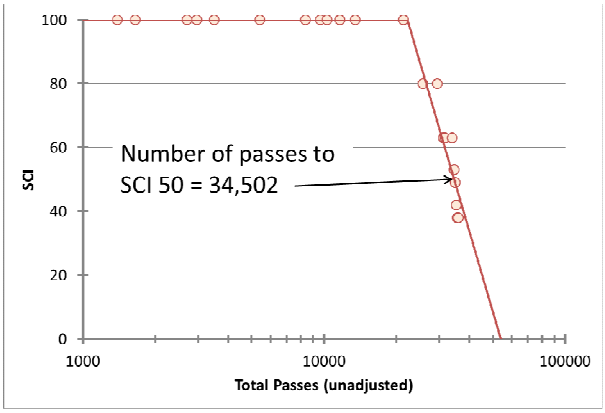

(d) MRS-2 South

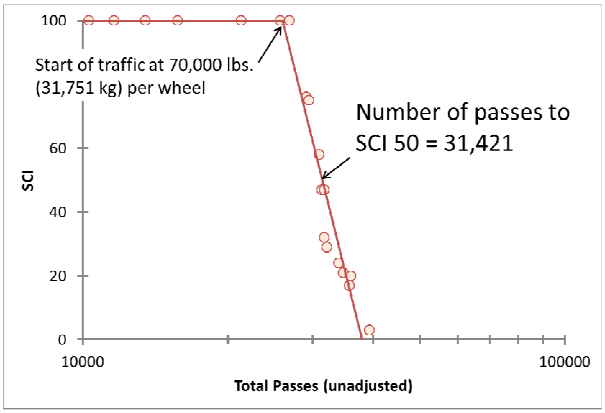

(e) MRS-3 North

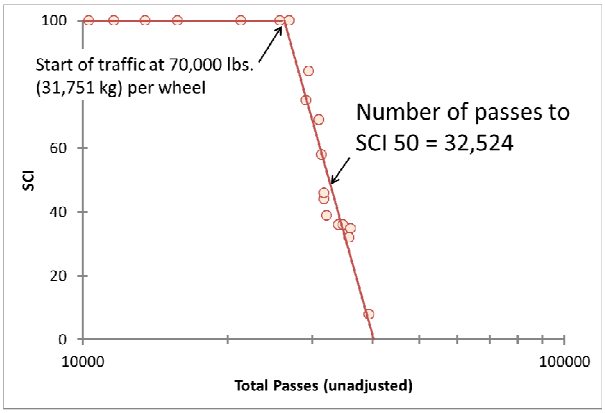

(f) MRS-3 South

Figure 6. SCI as a function of total passes for all six CC6 test items.

ANALYSIS AND DISCUSSION

Table 7 shows that when compared on the basis of equivalent passes at a reference load, the six CC6 rigid pavement test items are clearly differentiated by the concrete strength, with higher strength corresponding to longer equivalent life. Regardless of the reference load used, the MRS-3 test items (high-strength concrete) had much longer structural life than the corresponding MRS-2 test items (medium-strength) of equal cross section, which in turn had longer life than the MRS-1 items (low-strength). This result does not contradict the observation, discussed in the introduction, that high-strength concrete exhibits relatively more brittle failure behavior than normal-strength concrete. However, it does suggest that, within the range of practical concrete pavement strengths, brittle effects will not cause a reduction in rigid pavement fatigue life under aircraft traffic. In particular, no "optimal" concrete strength was identified from these full-scale tests. The results reconfirm that rigid pavement fatigue life is strongly correlated to the 28-day concrete strength, as assumed in the FAARFIELD design model.

Nevertheless, the observed increase in pavement life at high strength is not as great as predicted by the FAARFIELD failure model. From Table 7 (considering the 70,000-lb. wheel as the reference load) increasing the concrete strength from 660 to 1000 psi resulted in an overall increase in equivalent life from 85 to 4,731 passes on the north side, and from 25 to 5,832 passes on the south side – that is, by a factor of between 50 and 200 times. However, going from MRS-1 to MRS-2 resulted in an increase of between 12-50 times, while the corresponding increase going from MRS-2 to MRS-3 was only about 5 times. This is a significant difference, especially considering that the mean strength increase from MRS-2 to MRS-3 was approximately 250 psi, while the mean increase from MRS-1 to MRS-2 was less than 100 psi.

For comparison, some FAARFIELD 1.4 life predictions are given in Table 8. When concrete strength is increased from 660 to 750 psi, the ratio of predicted passes to failure is consistent with the range observed in CC6 for MRS-1 and MRS-2. By contrast, a strength increase from 750 to 1000 psi results in a much larger than observed increase in predicted life (Figure 7). The number of passes to failure as computed by FAARFIELD increases from 8 to 1089 passes, a factor of 136 – compared with 5-35 in the full-scale test. This indicates that the sensitivity of the FAARFIELD design model to changes in design concrete strength, particularly at high strength, may need to be re-evaluated in light of the CC6 results. Whether this particular model deviation from the observed result is evidence of brittle behavior, or is related to material factors unique to the CC6 experiment, has not been resolved. It should be noted that he "embrittlement" phenomenon is primarily a function of concrete strength itself, although Bažant and Planas indicate that material factors, such as aggregate shape and quality, can affect it as well [1]. The fact that a relatively small increase in strength (MRS-1 versus MRS-2) was accompanied by a large increase in the number of passes to failure, while a larger increase in strength (MRS-2 versus MRS-3) did not see a proportionately large performance increase may be attributable to the very different sources of increased strength. As indicated in a previous section, the difference in 28-day strength between the MRS-1 and MRS-2 mixes was due to a combination of factors, including better quality aggregates, while the additional increase in strength for MRS-3 was obtained mainly by increasing the cement factor relative to MRS-2. Since FAARFIELD's design model does not differentiate between the strength from high quality materials and that from adding cement, this may account for some of the discrepancy in life prediction discussed above.

Table 8.
Predicted Passes to Failure Based on FAARFIELD 1.4.

PCC Strength, psi	Wheel Load, lbs.	Predicted Life (Passes to Failure)[a]	Ratio
660	45,000	585	13
750	45,000	7551	
750	70,000	8	136
1000	70,000	1089	

[a]based on the MRS-1, -2 and -3 North sections, Table 1

Another significant observation from Table 7 and Figure 6 was the overall similarity in performance between north and south test items, as measured by SCI. In general, no significant difference in SCI versus traffic was observed for rigid test items on HMA bases (north test items) and econocrete bases (south test items). This is somewhat of an over-simplification of the actual test result, as significant qualitative differences in the crack patterns were observed, with a greater proportion of the total distress on econocrete-base test items being contributed by corner breaks, as opposed to longitudinal or transverse cracks. Thus, the use of a single number (SCI) to characterize performance may obscure some critical differences in structural behavior.

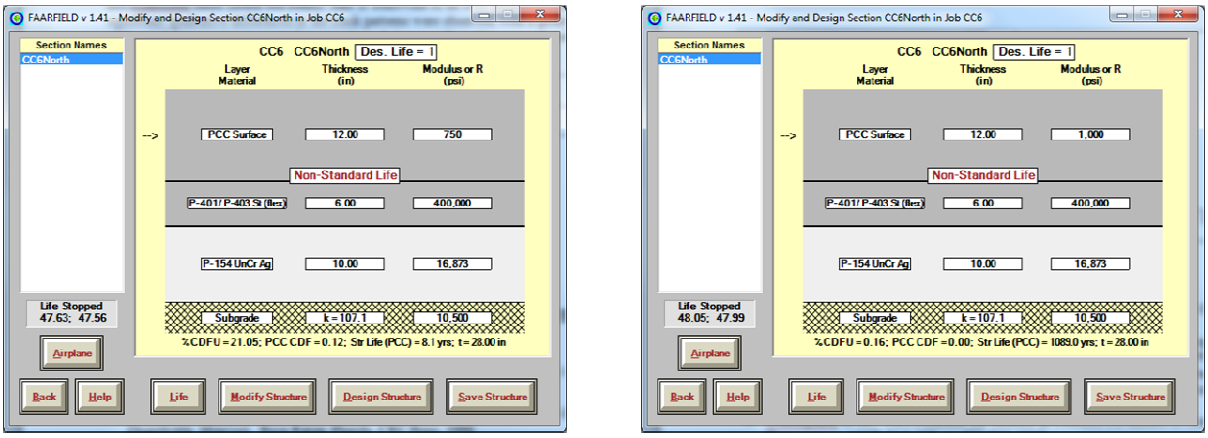

(a) R = 750 psi, Life = 8 passes (b) R = 1000 psi, Life = 1089 passes

Figure 7. FAARFIELD 1.4 comparative life computations for MRS-2 North and MRS-3 North test items. Load is NAPTF 2D gear at 70,000 lbs per wheel.

CONCLUSIONS

Ideally, full-scale traffic tests to failure should use a single type of vehicle load on all test items, which eliminates mixed traffic considerations in the subsequent analysis. This was not possible for the CC6 rigid pavement tests conducted at the FAA's NAPTF in 2011-2012, however, because of the significantly different concrete flexural strengths used for the six test items. After more than 15,000 passes of the NAPTF test vehicle at the initial load of 45,000 lbs. per wheel, only the two low-strength test items (MRS-1) exhibited significant distress, while the medium- and high-strength concrete test items were essentially undamaged. Higher loads were

then required to fail MRS-2 and MRS-3 test items. To account for the resulting mixed loading, a rational load compensation procedure was used, which converted all traffic to equivalent passes of a reference vehicle load.

When all test items were compared on the basis of equivalent passes at the reference load, it was apparent that test item performance always ranked according to 28-day concrete strength, with the high-strength test items at the top, the medium-strength in the middle, and low-strength test items at the bottom. Although it has been surmised that high concrete strength may lead to reduced fatigue life in rigid pavements due to embrittlement, this was not found to be the case for the mixes tested. When all traffic was converted to the 70,000-lb. wheel load, the high-strength test items allowed approximately five times more passes to failure than the medium-strength test items constructed with the same cross-section. While this ratio is less than the ratio of passes to failure predicted by the new FAARFIELD model, the CC6 results generally support the principle, embedded in the FAARFIELD design procedure, that concrete flexural strength is the major material property influencing rigid pavement life.

ACKNOWLEDGMENTS/DISCLAIMER

The work described in this paper was supported by the FAA Airport Technology R&D Branch, Michel J. Hovan, Manager. The contents of the paper reflect the views of the authors, who are responsible for the facts and accuracy of the data presented within. The contents do not necessarily reflect the views and policies of the FAA. This paper does not constitute a standard, specification or regulation

REFERENCES

1. Bažant, Zdeněk, and Planas, Jaime, *Fracture and Size Effect in Concrete and Other Quasibrittle Materials*, Boca Raton, Florida, CRC Press, 1998.
2. Tayabji, Shiraz, and Anderson, John, Principal Investigators, "A Proposed Specification for Construction of Concrete Airfield Pavement," Report IPRF-01-G-002-04-1, Innovative Pavement Research Foundation, Skokie, Illinois, July 2007.
3. Federal Aviation Administration, Office of Airport Safety and Standards, "Airport Pavement Design and Evaluation," Advisory Circular AC 150/5320-6E, 1999.
4. Brill, David R. and Wang, Qiang, "Analysis of Comparative Isolation Joint Tests at the FAA National Airport Pavement Test Facility," Proceedings of the 8th International DUT-Workshop on Research and Innovations for Design of Sustainable and Durable Concrete Pavements, Prague, Czech Republic, September 21 – 22, 2014 (accepted for publication).
5. Federal Aviation Administration, Office of Airport Safety and Standards, "Standards for Specifying Construction of Airports," Advisory Circular AC 150/5370-10F, 2011.
6. ASTM Standard ASTM C78 / C78M - 10e1, "Standard Test Method for Flexural Strength of Concrete (Using Simple Beam with Third-Point Loading)," ASTM International, West Conshohocken, PA, 2010, DOI: 10.1520/C0078_C0078M-10E01, www.astm.org.
7. Guo, Edward H., Brill, David R., and Yin, Hao, "Concrete Pavement Strength Investigations at the FAA National Airport Pavement Test Facility," Proceedings of the 7th RILEM International Conference on Cracking in Pavements: Mechanisms, Modeling, Testing, Detection, Prevention and Case Histories – Volume 1, Delft, Netherlands, June 20-22, 2012.

A. Scarpas, N. Kringos, I. al-Qadi and A. Loizos, editors, RILEM Bookseries, Springer, 2012.

8. ASTM Standard ASTM D5340 - 12, "Standard Test Method for Airport Pavement Condition Index Surveys," ASTM International, West Conshohocken, PA, 2010, DOI: 10.1520/D5340-12, 2012, www.astm.org.
9. Hayhoe, Gordon F., and Kawa, Izydor, "Methodology for Temperature and Load Compensation in Full-Scale Traffic Tests on Flexible Airport Pavements," Proceedings of the Ninth International Conference on the Bearing Capacity of Roads, Railways and Airfields – Volume 1, Trondheim, Norway, June 25-27, 2013. I. Hoff, H. Mork and R.G. Saba, editors, Trondheim, Norway, Akademika Publishing, 2013.
10. Brill, David R., *Calibration of FAARFIELD Rigid Pavement Design Procedure*, Technical Report DOT/FAA/AR-09/57, Washington, DC, Federal Aviation Administration, Office of Airport Safety and Standards, 2010.
11. Brill, David R., "Update on CC6," presentation to the FAA Airport Pavement Working Group Meeting, Atlantic City, New Jersey, 2012.